Dynamics of Micro-Air-Vehicles with Flapping Wings: A Multibody System Approach

B. A. Roccia, S. Preidikman, C. G. Gebhardt and J. C. Massa

Abstract— **This paper presents the development of a dynamic model to study the flight mechanics of a micro-air-vehicle with flapping wings. This model is based on Lagrange's equations for constrained systems. The micro-air-vehicle is modeled as a collection of three rigid bodies (a central body and two wings). The wings have prescribed motions relative to the central body, i.e., they are kinematically driven. The numerical integration of all the governing equations, which are differential-algebraic, is performed simultaneously and interactively in the time domain. The integration scheme couples a 4^{th}-order predictor-corrector method, the modified method of Hamming, with a procedure to stabilize the resulting differential-algebraic equations.**

Keywords— **multibody system, MAV, flapping wings.**

I. Introduction

RECENTLY, researchers and specialist in different areas of science have focused on the study and design of Micro-Air-Vehicles (MAVs) inspired by biology. The development of this new class of vehicles is motivated by numerous civilian and military applications that these apparatus will be able to perform. Such applications involve surveillance missions, inspection of collapsed buildings, exploration of dead-dirty-dangerous environments, among others. A vehicle capable of carrying out such missions, in indoors and outdoors environments, should exhibits extraordinary abilities to maneuver, avoid obstacles, navigate at low speeds, switch quickly between forward and hovering flight, and to move efficiently in reduced spaces. All these requirements make attractive the idea of using flapping-wings to design a functional MAV, filling a niche left by conventional fixed and rotary wings.

Nevertheless, there are still major technical barriers to be overcome such as: energy generation and storage; light materials; miniaturization of sensors, actuators and high-accuracy processing units of low power; understanding of unsteady aerodynamics at low Reynolds numbers; development of mechanisms that can be sharply controlled to bend and twist the wings at appropriate frequencies; and the capability of design wings with adequate size, shape and flexibility to maximize lift and minimize energy consumption.

Another important issue is to develop an accurate dynamic model to study the flight stability of these vehicles and predict their behavior in different flight configurations as well as diverse flow conditions. However, a complete dynamic model of such vehicles remains a challenge because the high nonlinear-unsteady aerodynamics, variable mass properties, and highly-nonlinear motions that characterize the flight at small scale (flying insects and small birds).

The research in the flapping wing field has greatly increased over the last ten years, especially in aerodynamics [1]. Studies on dynamics of MAVs with the flapping-wing concept are generally addressed by using standard aircraft equations with six degrees of freedom [2]. This technique was used by several researchers to conduct studies on the dynamics of different species of insects and various prototypes of MAVs [3, 4 y5]. However, in all these works, the mass of the wings and the associated inertial effects were neglected due to the small relative mass respect to the rest of the body.

Later, Grauer and Hubbard derived the equations of motion of an ornithopter using the Boltzman-Hamel equations [6]. They modeled the MAV as five rigid bodies: one for the central body, one for each wing, and two for the tail. Recently, Orlowski and Girard used an approach based on multibody dynamics to derive the non-linear equations of motion of a flapping-wing micro-air-vehicle [7] to carry out a comprehensive study of the influence of the wings mass on the MAV body. They showed that when the mass of the wings is decreased relative to the body mass, their numerical results approach to the results given by the standard aircraft model.

In this paper, we study the flight dynamics of a flapping-wing micro-air-vehicle by means of: *i*) an aerodynamic model based on the nonlinear-unsteady vortex-lattice method (UVLM); and *ii*) a dynamical model for the MAV founded on a multi-body system approach. The coupling between the two models is strong, since aerodynamic loads "deform" the set of rigid bodies that make up the vehicle, and reciprocally, this "deformation" modifies the aerodynamic loads acting on wing surfaces. Although for the flight mechanics of MAVs, it is very important to model correctly the coupling between aerodynamics and dynamics, in this paper, as a first stage, we use a decoupled version in order to separately test, verify and validate the dynamic model.

II. Geometry of the MAV

The computational model of the micro-air-vehicle adopted in this paper to study the dynamics of flapping-wings is based on the fruit fly (*Drosophila melanogaster*) morphology [8]. For simplicity, we modeled each part of the central body, the fuselage, as a revolution surface (see Fig. 1). The revolution surfaces that define the body as well as the wing surfaces were discretized using simple quadrilateral elements with four nodes. The reasons for this discretization are explained in section IV.

B. A. Roccia, Cordoba National University, Córdoba, Argentina, broccia@ing.unrc.edu.ar
S. Preidikman, Córdoba National University, Córdoba, Argentina, spreidik@umd.edu
C. G. Gebhardt, Cordoba National University, Córdoba, Argentina, cggebhardt@yahoo.com.ar
J. C. Massa, Córdoba National University, Córdoba, Argentina, .jmass@efn.uncor.edu

III. Aerodynamic Model

In this work, we used an enlarged and modified version of the general method known as unsteady vortex-lattice method. This method can be applied to three-dimensional lifting and non-lifting flows. The surface of the body may undergo arbitrary time-dependent deformation, and it can execute any type of maneuver in the space surrounded by moving air. The flow around the full body, i.e. the fuselage and wings of the MAV, is assumed to be irrotational and incompressible over the entire flowfield, except surrounding regions of the solid boundaries of the body and wakes. As a result of the relative motion between the body and the fluid, vorticity is generated in a thin region surrounding the surface of the body (the boundary layer). Part of this vorticity is shed from the sharp edges and forms the wakes. We consider the boundary layers and wakes as zero-thickness sheets of vorticity.

The proposed model considers a flow of an incompressible fluid characterized by a very high Reynolds number. The governing equation is the well-known Laplace's equation of continuity for incompressible and irrotational flows:

$$\nabla^2 \psi(\mathbf{x}, t) = 0\,, \tag{1}$$

where $\psi(\mathbf{x},t)$ is the velocity potential function, which is valid in the whole irrotational and incompressible fluid domain (outside of the boundary layers and the wakes), $\mathbf{x}$ is the position vector and t is time.

The time dependence is introduced in Laplace's equation by the boundary conditions. In the fluid domain the vorticity field $\boldsymbol{\Omega}$ and the velocity field $\mathbf{V}$ co-exist.

In the case of a finite straight vortex segment of circulation $\Gamma(t)$ the velocity associated can be computed using the following discrete version of the Biot-Savart law:

$$\mathbf{V}(\mathbf{x},t) = \frac{\Gamma(t)}{4\pi} \frac{\boldsymbol{\omega}(\mathbf{x},t)\times\mathbf{x}_1}{\left\| \boldsymbol{\omega}(\mathbf{x},t)\times\mathbf{x}_1 \right\|_2^2} \left[\boldsymbol{\omega}(\mathbf{x},t)\cdot(\hat{\mathbf{e}}_1 - \hat{\mathbf{e}}_2) \right], \tag{2}$$

where $\mathbf{x}_1$ and $\mathbf{x}_2$ are the position vectors of the point where the velocity are computed relative to the ends of the straight vortex segment, $\hat{\mathbf{e}}_1$ and $\hat{\mathbf{e}}_2$ unit vectors associated to $\mathbf{x}_1$ and $\mathbf{x}_2$ vectors, and $\boldsymbol{\omega} = \mathbf{x}_1 - \mathbf{x}_2$.

A. Discretization of the vortex sheets

In the unsteady vortex-lattice method, we replace the bound-vortex sheets by a lattice of short, straight vortex segments of circulation $\Gamma_i(t)$. These segments divide the surface of the insect's body and insect's wings into a number of elements of area (panels). The model is completed by joining free vortex lines, representing the free-vortex sheets, to the bound-vortex lattice along the edges of separation; such as the trailing edges and leading edges of the lifting surfaces.

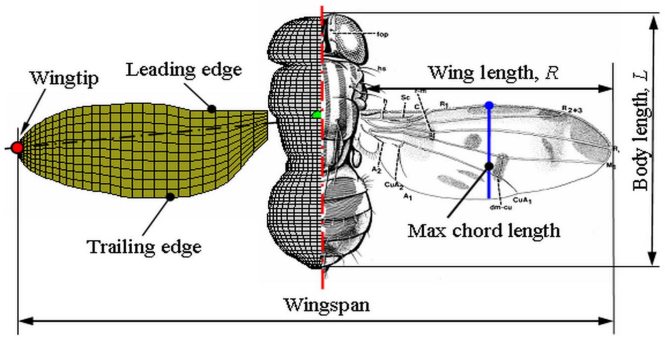

Figura 1. Computational model of the MAV and MAV dimensions based on morphological parameters of a fruit fly.

B. Boundary conditions

The governing equation of the problem is complemented with the following boundary conditions:

1) *Regularity at infinity*: this condition requires that all disturbances due to a moving body in a fluid, initially at rest, decay away from body and its wakes.

2) *The non-penetration condition*: it is applied over the entire boundary of the solid immersed in the fluid. This condition also called of impermeability requires that the normal component of the velocity of all fluid particles relative to the body surface must be zero on the body surface. This condition is imposed on control points located in the geometric center of each panel.

C. Aerodynamics loads

The aerodynamics loads on the lifting surfaces (MAV's wings) are computed as follows: *i*) for each element the pressure jump at the control point is computed with the unsteady Bernoulli equation (3); *ii*) the force in each element is computed as the product of the pressure jump times the element area times the normal unit vector; *iii*) the resultant forces and moments are computed as the vector summation of the forces and moments produced by each element.

$$\frac{\partial}{\partial t}\psi(\mathbf{x},t) + \frac{1}{2}\mathbf{V}(\mathbf{x},t)\cdot\mathbf{V}(\mathbf{x},t) + \frac{p(\mathbf{x},t)}{\rho} = H(t)\,, \tag{3}$$

where $\mathbf{V}(\mathbf{x},t)$ is the absolute velocity, the spatial gradient of ψ, $p(\mathbf{x},t)$ is the unknown pressure, ρ is the constant density of the fluid, and H is the energy per mass unit which is a function of time.

For a detailed mathematical formulation of the unsteady lattice-vortex method, the reader may consult [9].

IV. Dynamic Model

The MAV is modeled as a system of three rigid bodies (n_b=3), a central body and two wings. The dynamic equations of motion for the MAV are derived by means of Lagrange's equations for constrained systems. The location of each body in space is identified by using a set of six absolute generalized coordinates (three coordinates define the position of a fixed point on the

body and three define its orientation). It makes a total of eighteen generalized coordinates ($6n_b = 18$), which are not independent, these are linked through constraint equations. The wings have a prescribed motion (kinematically driven) with respect to the central body. This fact introduces twelve constraint equations (n_c = 12), six to specify the joint point between the central body and the wings and another six to specify the orientation of the wings with respect to the central body. Thus, the number of degrees of freedom of the multibody system is six ($n_{\text{dof}} = 6n_b - n_c = 6$).

In this work, we used four reference systems (see Fig. 2): *i*) a Newtonian or inertial system **N**; and *ii*) a reference system fixed to each body of the MAV $\mathbf{B}_i$. To orientate each body with respect to the inertial frame, we used a rotation representation based on Euler angles, a (2-3-1) rotation sequence for the central body and a (1-3-2) rotation sequence for each wing.

The set of the absolute generalized coordinates for each body are

$$\mathbf{q}_i = \left(x_i,\, y_i,\, z_i,\, \phi_i,\, \theta_i,\, \psi_i\right)^T, \quad \text{for } i = 1,2,3, \tag{4}$$

where x_i, y_i, and z_i are rectangular Cartesian coordinates associated to the unitary vectors $\hat{\mathbf{n}}_1$, $\hat{\mathbf{n}}_2$ and $\hat{\mathbf{n}}_3$ respectively, and ϕ_i, θ_i, ψ_i are angular coordinates which orientate each body relative to the inertial frame **N**.

A. Constraint Equations

For each wing, we have two different constraint equations:

1) *Position constraint*: it specifies the joint point between the wings and the central body; and
2) *Orientation constraint*: it specifies the orientation of each wing with respect to the central body.

All constraint equations are written with respect to the inertial reference frame **N**. Equation (5) presents the constraint equations for the left wing only. Constraint equations for the right wing are obtained with the same procedure. These are:

$$\begin{aligned}
\varphi_i &= \left(\mathbf{R}_2 - \mathbf{R}_1 - \mathbf{T}_{\mathbf{NB}_1}\mathbf{r}_{rai}\right)\cdot\hat{\mathbf{n}}_i = 0, \quad \text{for } i = 1,2,3,\\
\varphi_4 &= \left(\hat{\mathbf{b}}_1^2\right)^T\left(\mathbf{T}_{\mathbf{NB}_2}^T\mathbf{T}_{\mathbf{NB}_1}\mathbf{S}(t)\right)\hat{\mathbf{a}}_2 = 0,\\
\varphi_5 &= \left(\hat{\mathbf{b}}_2^2\right)^T\left(\mathbf{T}_{\mathbf{NB}_2}^T\mathbf{T}_{\mathbf{NB}_1}\mathbf{S}(t)\right)\hat{\mathbf{a}}_3 = 0, \text{ and,}\\
\varphi_6 &= \left(\hat{\mathbf{b}}_3^2\right)^T\left(\mathbf{T}_{\mathbf{NB}_2}^T\mathbf{T}_{\mathbf{NB}_1}\mathbf{S}(t)\right)\hat{\mathbf{a}}_1 = 0.
\end{aligned} \tag{5}$$

where $\mathbf{R}_i$ for i = 1,2,3 is the position vector of the origin of the reference frame fixed to each part of the multibody system with respect to the inertial frame **N** (see Fig. 2), $\mathbf{T}_{\mathbf{NB}i}$ for i = 1,2,3 represents the coordinate transformation matrix between the reference frame $\mathbf{B}_i$ and the inertial frame **N**, $\mathbf{r}_{rai}$ is the position vector of the joint point between the left wing and central body with respect to the reference frame $\mathbf{B}_2$ fixed to the central body, $\mathbf{S}(t)$ is a rotation matrix which orients the left wing with respect to the central body and it depends of the

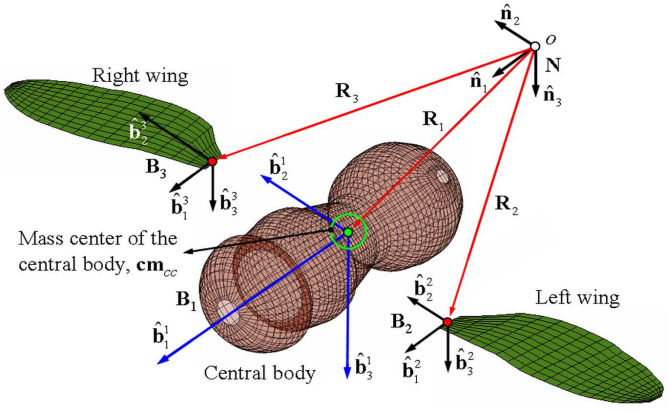

Figura 2. Reference systems attached to each body of the multibody system.

adopted kinematic description for the motion of the wings during a stroke cycle [10], and the unit vectors $\hat{\mathbf{a}}_i$ for i = 1,2,3 forms an additional reference frame called **A** which results from composing the rotations $\mathbf{S}(t)$ and $\mathbf{T}_{\mathbf{NB_1}}$.

Finally, the constraint vector $\mathbf{\Phi}(\mathbf{q}, t)$ can be expressed as

$$\mathbf{\Phi}(\mathbf{q}, t) = \left(\varphi_1,\, \varphi_2, \ldots, \varphi_{12}\right)^T, \tag{6}$$

where $\mathbf{q} = (\mathbf{q}_1, \mathbf{q}_2, \mathbf{q}_3)^T$.

Position constraint equations as well as orientation constraint equations are both holonomics. In particular, the first ones are scleronomics because the time variable does not appear explicitly in the formulation. On the contrary, the last ones are rheonomics because the prescribed motion of the wings introduces an explicitly time dependence which is reflected by the rotation matrix $\mathbf{S}(t)$ in (5) [10].

B. Generalized Loads

The generalized loads associated with the set of absolute generalized coordinates are calculated using the principle of virtual work [11]. These loads may be of very different nature. In this work we consider two kinds of forces: *i*) the forces that arise from the aerodynamics (non-conservatives); and *ii*) the forces due to the action of the terrestrial gravitational field (conservatives). The virtual work of an external force, **F**, applied to the system can be expressed as

$$\delta W = \mathbf{F}\cdot\delta\mathbf{r}, \tag{7}$$

where $\delta\mathbf{r}$ is an admissible virtual displacement contained in the tangent space $\mathrm{T}_{\mathbf{r}}\mathrm{M}$ to the configuration space manifold M [12].

The virtual displacement of an arbitrary point belonging to the *i*-th body can be expressed as

$$\delta\mathbf{r} = \delta\mathbf{R}_i + \delta\left(\mathbf{T}_{\mathbf{NB}_i}\mathbf{r}\right). \tag{8}$$

Substituting (8) into (7) and making some manipulations we obtain the following general expression for the aerodynamic generalized loads associated to the *i*-th body, given by

$$\mathbf{Q}_i^{nc} = \sum_{j=1}^{np}\left({}^i\mathbf{F}_j\right)^T\begin{bmatrix}\mathbf{I}_3 & \mathbf{H}_j\end{bmatrix}, \quad \text{for } i = 2,3, \tag{9}$$

where $\mathbf{I}_3$ is the identity matrix 3x3, *np* is the number of panels in which each wing of the MAV has been discretized, ${}^{i}\mathbf{F}_j$ is a vector force acting on the area center of the *j*-th aerodynamic panel belonging to the *i*-th body, and $\mathbf{H}_j$ is a matrix of 3x3 obtained by evaluating the partial derivative of $\mathbf{T}_{\mathbf{NB}_i}\mathbf{r}$ with respect to the vector of generalized coordinates $\mathbf{q}_i$.

The generalized loads due to the terrestrial gravitational field are obtained with a similar procedure. Therefore, the mathematical expression for this term is given by

$$\begin{aligned} \mathbf{Q}_1^g &= \left({}^{1}\mathbf{F}_g\right)^T \mathbf{I}_3, \\ \mathbf{Q}_i^g &= \left({}^{i}\mathbf{F}_g\right)^T \begin{bmatrix}\mathbf{I}_3 & \mathbf{H}_i\end{bmatrix}, \quad \text{for } i = 2,3, \end{aligned} \tag{10}$$

where ${}^{i}\mathbf{F}_g = m_i g\,\hat{\mathbf{n}}_3$, m_i is the mass of the *i*-th body and *g* is the gravity acceleration constant.

C. Equations of motion

The equations of motion for the MAV are derived by means of an energetic formulation based on Lagrange's equations for constrained systems. In this work, the potential due to the gravitational field is directly included into the term of generalized loads (see subsection IV.B). Thus, Lagrange's equations take the following form:

$$\begin{aligned} &D_t\left(\partial_{\dot{\mathbf{q}}}\, T\right) - \partial_{\mathbf{q}}\, T + \mathbf{B}_{\mathbf{q}}^T\,\boldsymbol{\lambda} = \left(\mathbf{Q}^{nc}\right)^T + \left(\mathbf{Q}^{c}\right)^T, \\ &\boldsymbol{\Phi}\left(\mathbf{r},t\right) = \mathbf{0}, \end{aligned} \tag{11}$$

where $(\dot{\ })$ denotes the first time derivative, D_t denotes the total time derivative, $\partial_{\mathbf{x}}$ denotes the partial derivative with respect to the vector $\mathbf{x}$, *T* is the kinetic energy of the system, $\boldsymbol{\lambda}$ is the vector of Lagrange's multipliers, $\mathbf{B}_{\mathbf{q}}$ is the n_cx$6n_b$ Jacobian Matrix of constraints, $\mathbf{Q}^{nc} = \left(\mathbf{Q}_1^{nc}, \mathbf{Q}_2^{nc}, \mathbf{Q}_3^{nc}\right)$ and $\mathbf{Q}^{c} = \left(\mathbf{Q}_1^{g}, \mathbf{Q}_2^{g}, \mathbf{Q}_3^{g}\right)$.

Using the methodology proposed by Shabana [13], the kinetic energy of the *i*-th body can be expressed as

$$T_i = \frac{1}{2}\mathbf{q}_i^T\,\mathbf{M}_i\,\mathbf{q}_i, \tag{12}$$

where matrix $\mathbf{M}_i$ represents the generalized mass and inertia properties of the *i*-th body and it is dependent upon the rotation parameterization adopted to describe its orientation in space.

Introducing (12) into (11) we obtained the equations of motion for the *i*-th body,

$$\mathbf{M}_i\,\ddot{\mathbf{q}}_i + \mathbf{B}_{\mathbf{q}_i}^T\,\boldsymbol{\lambda} = \mathbf{Q}_i^{v} + \left(\mathbf{Q}_i^{nc}\right)^T + \left(\mathbf{Q}_i^{c}\right)^T, \tag{13}$$

where $\mathbf{Q}_i^{v}$ is a quadratic velocity vector that arises from differentiating the kinetic energy with respect to time and with respect to the generalized coordinates of the *i*-th body.

This quadratic velocity vector is given by,

$$\mathbf{Q}_i^{v} = -\,\dot{\mathbf{M}}_i\,\dot{\mathbf{q}}_i + \partial_{\mathbf{q}_i}\,T_i. \tag{14}$$

Finally, the equations of motion for the complete multibody system are obtained by assembling the equations of motion for each body complemented with constraint equations, as

$$\begin{aligned} &\mathbf{M}\,\ddot{\mathbf{q}} + \mathbf{B}_{\mathbf{q}}^T\,\boldsymbol{\lambda} = \mathbf{Q}^{v} + \left(\mathbf{Q}^{nc}\right)^T + \left(\mathbf{Q}^{c}\right)^T, \\ &\boldsymbol{\Phi}\left(\mathbf{r},t\right) = \mathbf{0}. \end{aligned} \tag{15}$$

The term $\mathbf{B}_{\mathbf{q}}^T\boldsymbol{\lambda}$ represents the generalized constraint forces, *i.e.*, a force acting in the configuration space. The meaning of each multiplier depends on the specific manner in which the constraint was written [11].

V. Numerical Simulations

The differential equations and the vector of kinematic constraints in (15) represent a system of *differential-algebraic equations* (DAEs) of index three for the multibody system. These dynamic equations are, in general, nonlinear and a close-form solution for these equations is often difficult to obtain. To solve the governing equations (15) we differentiate the constraints twice. This new equation is often called *constraint acceleration level* and is given by,

$$\ddot{\boldsymbol{\Phi}} \;=\; \mathbf{B}_{\mathbf{q}}\ddot{\mathbf{q}} + \partial_{\mathbf{q}}\left(\mathbf{B}_{\mathbf{q}}\dot{\mathbf{q}}\right)\dot{\mathbf{q}} + 2\partial_{\mathbf{q}}\left(\partial_t\boldsymbol{\Phi}\right)\dot{\mathbf{q}} + \partial_{tt}\boldsymbol{\Phi} \;=\; \mathbf{0}, \tag{16}$$

where ∂_t and ∂_{tt} denotes first and second partial time derivatives.

The set of ordinary differential equation in (15) is written together with (16) as an index-1 DAE,

$$\begin{bmatrix}\mathbf{M} & \mathbf{B}_{\mathbf{q}}^T \\ \mathbf{B}_{\mathbf{q}} & \mathbf{0}_{12}\end{bmatrix}\begin{Bmatrix}\ddot{\mathbf{q}} \\ \boldsymbol{\lambda}\end{Bmatrix} = \begin{Bmatrix}\mathbf{Q}^{v} + \left(\mathbf{Q}^{nc}\right)^T + \left(\mathbf{Q}^{c}\right)^T \\ \mathbf{U}\left(\mathbf{q},\dot{\mathbf{q}},t\right)\end{Bmatrix}, \tag{17}$$

where $\mathbf{U}\left(\mathbf{q},\dot{\mathbf{q}},t\right) = -\partial_{\mathbf{q}}\left(\mathbf{B}_{\mathbf{q}}\dot{\mathbf{q}}\right)\dot{\mathbf{q}} - 2\partial_{\mathbf{q}}\left(\partial_t\boldsymbol{\Phi}\right)\dot{\mathbf{q}} - \partial_{tt}\boldsymbol{\Phi}$ and $\mathbf{0}_{12}$ is a null matrix of 12x12.

Equation (17) may be integrated using standard codes for ODEs. However, there are serious problems associated with the numerical integration of (17). The easily visible one is that the position and velocity constraints are no longer satisfied exactly – there is a drift off the constraints, which does not look good in a graphical depiction of motion simulation. Moreover, the drift magnitude as well as the error in generalized positions and velocities grows with time – at worst quadratically. This is not because of the numerical method used to integrate (17) but because the system (17) itself is mildly unstable [14, 15].

In the bibliography it can be found several stabilization methods to correct this numerical drift, among which the most widely used because its simplicity is Baumgarte's technique [16]. However this technique may get into trouble in difficult situations and the choice of the parameters involved in it has proved to be tricky in practice. Another technique currently used to stabilize (17) is based on the projection of the solution onto the constraint manifold (or part of it). There are two basic ways to perform this projection, one of them consists in redefining the ODE by adding new Lagrange's multipliers (*projected invariants*), and the other approach consists in discretizing numerically the ODE and at the end of each discretization step to project the approximate solution onto the selected constraints manifold (*coordinate projection*) [17]. In this work, we adopted the coordinate projection method to eliminate the numerical drift that arises during the numerical integration of the index-1 DAE (17).

A. Integration scheme and stabilization method

The approach followed in this work treat the airflow and the structure as elements of a single dynamical system and integrate all the governing equations numerically, simultaneously, and interactively in the time domain. Although the coupling between the aerodynamic and the dynamic model is been developed, we prefer to implement a numerical procedure able to deal efficiently with this problem in the future. The adopted procedure is based on Hamming's fourth-order predictor-corrector method [9]. This scheme was chosen for two reasons: *i*) the aerodynamic model behaves better when the loads are evaluated at integral time steps, and *ii*) the aerodynamic loads contain contributions that are proportional to the accelerations, therefore it is necessary to use methods that can treat those contributions on both sides of the equations.

Once the solution is computed by Hamming's method, it is projected onto both, the position and velocity constraint manifold **h**. Such a projection is performed by the following scheme:

$$\begin{Bmatrix}\mathbf{q}_{n+1}\\ \dot{\mathbf{q}}_{n+1}\end{Bmatrix}=\begin{Bmatrix}\tilde{\mathbf{q}}_{n+1}\\ \dot{\tilde{\mathbf{q}}}_{n+1}\end{Bmatrix}-\alpha\,\mathbf{F}\left(\tilde{\mathbf{q}}_{n+1},\dot{\tilde{\mathbf{q}}}_{n+1},t_{n+1}\right)\mathbf{h}\left(\tilde{\mathbf{q}}_{n+1},\dot{\tilde{\mathbf{q}}}_{n+1},t_{n+1}\right), \quad (18)$$

where,

$$\mathbf{h}\left(\mathbf{q},\dot{\mathbf{q}},t\right)\;=\;\begin{Bmatrix}\boldsymbol{\Phi}\left(\mathbf{q},t\right)\\ \mathbf{B}_{\mathbf{q}}\dot{\mathbf{q}}+\partial_t\boldsymbol{\Phi}\left(\mathbf{q},t\right)\end{Bmatrix}=\mathbf{0}, \quad (19)$$

form an invariant set of the ODE (17) and the solution $\left(\tilde{\mathbf{q}}^T,\dot{\tilde{\mathbf{q}}}^T\right)^T$ is computed by Hamming's method at $t=t_{n+1}$.

The stabilization scheme (18) has the desired stability behavior if **HF** is positive definite (where $\mathbf{H}=\partial_{\mathbf{q}}\mathbf{h}$). For the mechanical system under study, the constraint manifold results asymptotically stable for $0<\alpha<2$, and the choice $\alpha=1$ (which certainly depends on the discretization step size *h*), is close to be optimal. In addition, the stabilization matrix **F** defined as

$$\mathbf{F}\;=\;\mathbf{B}_{\mathbf{q}}^T\left(\mathbf{B}_{\mathbf{q}}\;\mathbf{B}_{\mathbf{q}}^T\right)^{-1}\begin{bmatrix}\mathbf{I}_{12} & \mathbf{0}_{12}\\ \mathbf{0}_{12} & \mathbf{I}_{12}\end{bmatrix}, \quad (20)$$

renders a good compromise between the requirements of efficiency and stability (procedure (18) together the definition (20) for the stabilization matrix **F** form a post-stabilization method which is denoted *S-both*). More details about the stability of scheme (18) as well as the selection criteria for the matrix **F** can be found in the works of Petzold [17, 18].

Another important issue to control or to completely eliminate constraint violations is to start an integration process with a set of initial conditions on the coordinates and velocities that satisfy their corresponding constraints. To find an adequate set of initial conditions we used the procedure described by Nikravesh [19] which is based on a partition of coordinates and velocities into dependent and independents sets. It is important to mention that this method does not consider any correction in the estimated values of the independent variables. Therefore, the kinematics constraints at coordinate and velocity levels are restated as

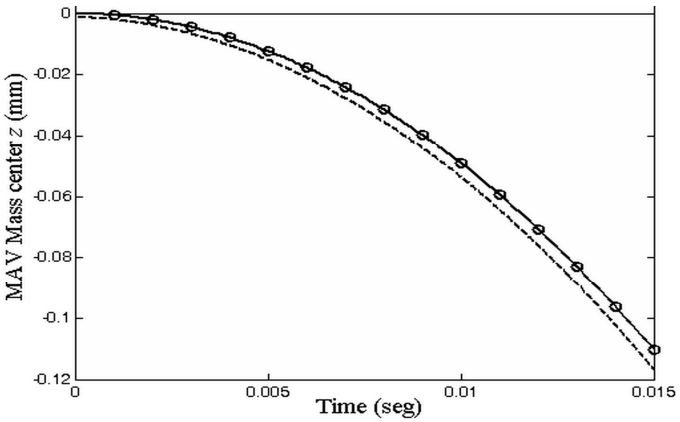

Figura 3. Verification of the dynamic model: circle dots for the formula $1/2gt^2$, solid line for the current model with no prescribed motion and dashed line for the current model with prescribed motion.

$$\boldsymbol{\Phi}\left(\mathbf{q}_{(ind)},\mathbf{q}_{(dep)},t\right)=\mathbf{0}\,, \quad (21)$$

and

$$\begin{bmatrix}\mathbf{B}_{\mathbf{q}}^{(dep)} & \mathbf{B}_{\mathbf{q}}^{(ind)}\\ \mathbf{0} & \mathbf{I}_{(ind)}\end{bmatrix}\begin{Bmatrix}\dot{\mathbf{q}}_{(dep)}\\ \dot{\mathbf{q}}_{(ind)}\end{Bmatrix}\;=\;\begin{Bmatrix}-\partial_t\boldsymbol{\Phi}\\ \dot{\mathbf{q}}_{(ind)}\end{Bmatrix}, \quad (22)$$

where (*ind*) denotes independent coordinates, (*dep*) denotes dependent coordinates, $\mathbf{B}_{\mathbf{q}}^{(dep)}$ is selected to be a nonsingular $n_c \times n_c$ matrix, $\mathbf{B}_{\mathbf{q}}^{(ind)}$ is an $n_c \times (6n_b - n_c)$ matrix and $\mathbf{I}_{(ind)}$ represents an $n_{\text{dof}} \times n_{\text{dof}}$ identity matrix.

The equation set (21) is solved iteratively by the Newton-Raphson method, and the set (22) is solved as a set of linear algebraic equations. This type of coordinate and velocity correction can be found in a variety of forms in the literature.

B. Preliminary numerical results

In this section, we present some results obtained with the numerical tool that we developed. Data reported by Bos *et al.* [20] on the actual kinematics of a fruit fly (*drosophila melanogaster*) in hover were used to describe the pattern of wing motion over a flapping cycle. The setup of the numerical experiment shown in this section consists of: *i*) a flapping frequency $n_f = 200$ Hz; *ii*) a wing length $R = 2.5$ mm and wing area $S = 2.21$ mm^2; and *iii*) a fully-spatial discretization of the MAV of 3448 aerodynamic panels.

First, we tested the current dynamic model to assess its validity and limitations. For this, we suppress the aerodynamic forces acting on the wing surfaces and the prescribed motion of the wings with respect to the central body, thus leaving the MAV in free fall. Figure 3 shows that the vertical path predicted by the current model exactly matches the results obtained by the simple formula, $\frac{1}{2}gt^2$, found in any basic physics textbook. On the other hand, if we add a prescribed motion of the wings, small differences can be observed with respect to the previous curves. This phenomenon occurs because an initial velocity of the wings results in an initial velocity on the whole mechanical system (in this case downwards).

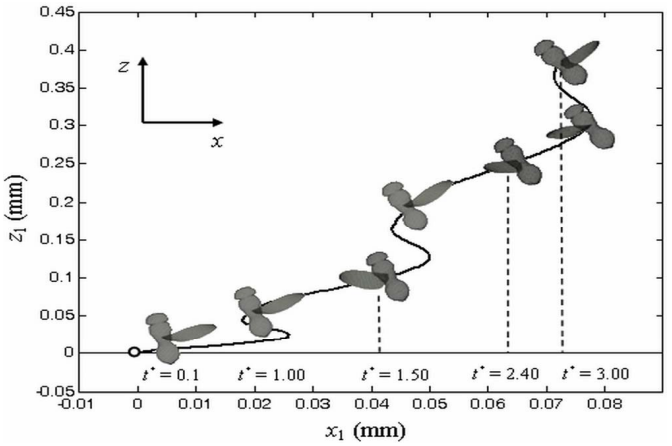

Figura 4. Path of the central body mass center for three complete wingbeat cycles. Dimensionless time shown in figure is related to dimensional time through the flapping frequency, $t = t^*/n_f$.

Figure 4 shows the simulated flight path of the central body mass center superimposed with silhouettes of the MAV configuration at several points in time.

The set of aerodynamic forces used as input for the current dynamic model allows the MAV remain aloft (also it can be seen a small rise of it). However, while the MAV rises, it can be observed that the pitch angle decreases. If this phenomenon continues, the flight becomes unstable and the MAV will crash. This fact is due to the lack of control elements for stabilizing the flight, allowing the MAV navigate properly.

Lateral displacement as well as yaw and roll angles are null because the wing movement is symmetric with regard to the plane defined by the unit vectors $\hat{\mathbf{n}}_1$ and $\hat{\mathbf{n}}_3$ (sagittal plane, see Fig. 2). On the other hand, the post-stabilization method chosen to control the numerical drift showed remarkable results with respect to other stabilization methods such as Baumgarte's technique. Moreover, the chosen stabilization matrix **F** showed better performance than other possible choices.

VI. Conclusions

In this paper we developed the dynamic equations of motion for a flapping-wing micro-air-vehicle. The dynamic model was formulated by using Lagrange's equations for constrained systems. Moreover, this model takes into account the contribution of the inertial effects of the wings on the central body (fuselage) of the MAV, effect that has been neglected in most of the works found in the literature.

The numerical integration of the dynamical equations was performed successfully by means of a modified scheme proposed in this work. This modified scheme consists of the Hamming's fourth-order predictor-corrector method coupled with a post-stabilization procedure based on the coordinate projection.

The model was validated by comparing its results with the simple formula for free fall found in any basic physics textbook. In addition, we presented results for the flight dynamics of a MAV in hovering and, although the aerodynamic and dynamic models still are decoupled, we obtained encouraging results.

Currently, we are developing an algorithm to combine the aerodynamic and dynamic model as a single dynamical system for solving all the governing equations through the numerical procedure proposed in this work.

References

[1] S. P. Sane, "The aerodynamic of insect flight," *J. Experimental Biology*, Aug. 2003, vol. 206, pp. 4191–4208.

[2] B. Etkin, and L. Reid, *Dynamics of Flight*, Wiley, New York, 1996.

[3] J. Dietl and E. Garcia, "Stability in ornithopter longitudinal flight dynamics," *J. of Guidance, Control, and Dynamics*, 2008, vol. 31, no. 4, pp. 1157–1162.

[4] X. Deng, L. Schenato, and S. Sastry, "Flapping flight for biomimetic robot insects: Part 2: Flight control design," *IEEE Trans. on Robotics and Automation*, 2006, vol. 22, no. 4, pp. 789–803.

[5] D. Doman, M. Oppenheimer, and D. Sigthorrson, "Dynamics and control of a minimally actuated biomimetic Vehicle: Part 2: Control," presented at the AIAA Guidance, Navigation, and Control Conference, Chicago, IL, *AIAA Paper* 2009-6161, 2009.

[6] J. Grauer and J. Hubbard, "Multibody model of an ornithopter," *AIAA J. of Guidance, Control, and Dynamics*, 2009, vol. 32, no. 5, pp. 1675–1679.

[7] C. T. Orlowski, and A. R. Girard, "Modeling and simulation of nonlinear dynamics of flapping wing micro air vehicles," *AIAA Journal*, 2011, vol. 49, no. 5, pp. 969–981.

[8] T. Markow and P. O'Grady, *Drosophila: A Guide to Species Identification and Use*, Elsevier Inc, San Diego CA, 2006.

[9] S. Preidikman, "Numerical simulations of interactions among aerodynamics, structural dynamics, and control systems," Ph.D. Dissertation, Dep. of Eng. Science and Mechanics, Virginia Tech, 1998.

[10] B. A. Roccia, S. Preidikman, J. C. Massa, and D. T. Mook, "Development of a kinematical model to study the aerodynamics of flapping-wings," *Int. J. of Micro Air Vehicles*, 2011, vol. 3, no. 2, pp. 61–88.

[11] O. A. Bauchau, *Flexible multibody dynamics*, Springer, New York, 2011.

[12] W. B. Heard, *Rigid Body Mechanics*, Wiley – VCH Verlag GmbH & Co., 2006.

[13] A. A. Shabana, *Dynamics of multibody systems*, Cambridge, New York, 2005.

[14] J. Yen, "Constrained equations of motion in multibody dynamics as ODEs on manifolds," *SIAM J. on Numerical Analysis*, Ap. 1993, vol. 30, no. 2, pp. 553–568.

[15] W. Blajer, "Elimination of constraint violation and accuracy aspects in numerical simulation of multibody systems," *Multibody System Dynamics*, vol. 7, pp. 265–284, 2002.

[16] P. Flores, M. Machado, and M. T. da Silva, "A parametric study on the Baumgarte stabilization method for forward dynamics of constrained multibody systems," *J. Comp. Nonlinear Dynamics*, Jan. 2011, vol. 6, pp. 011019-1–011019-9.

[17] U. M. Ascher, H. Chin, L. R. Petzold and S. Reich, "Stabilization of constrained mechanical systems with DAEs and invariant manifolds," *J. Mech. Struct. Machines*, 1995, vol. 23, pp. 135–158.

[18] U. Ascher, H. Chin, and S. Reich, "Stabilization of DAEs and invariant Manifolds," *Numer. Math*., vol. 67, pp. 131–149, 1994.

[19] P. E. Nikravesh, "Initial condition correction in multibody dynamics," *Multibody Syst. Dynamics*, 2007, vol. 18, pp. 107–115.

[20] F. M. Bos, D. Lentink, B. W. van Oudheusden and H. Bijl, "Numerical study of kinematic wing models of hovering insect flight," *45th AIAA Aerospace Sciences Meeting*, January 8-112007, Reno, Nevada.

Bruno Antonio Roccia received his BS degree in mechanical engineering in 2004, and his Master degree in 2009, both from Rio Cuarto National University in Argentina. He is currently Assistant Professor at Córdoba National University and also at Rio Cuarto National University. He is finishing his PhD at Córdoba National University. Professor Roccia is member of the SIAM, Society for Industrial and Applied Mathematics. His research interests include numerical methods in engineering, computational mechanics, multibody system dynamics, flapping wings, bioinspiration and biomimetics

Sergio Preidikman received his BS degree in aeronautical and mechanical engineering from the Universidad Nacional de Córdoba in 1988, his MS degree in civil engineering from the University of Puerto Rico in 1992, and his PhD in engineering mechanics from The Virginia Polytechnic Institute and State University in 1998. He is currently a Professor of Aeronautical and Mechanical Engineering at the Universidad Nacional de Córdoba, Argentina, and since 2006 and Associated Researcher at CONICET. He was a visiting Professor at the University of Maryland at College Park, USA and was an invited Researcher/Lecturer/Scholar at the Universities of Maryland at College Park, Texas at Brownsville, and the Virginia Polytechnic Institute and State University, USA, the Universidad de los Andes in Bogotá, the Universidad Nacional de Antioquia in Medellín and the Universidad del Cauca in Popayán, Colombia, at Åalborg University in Denmark, and at the University of Ottawa in Canada. Prior to joining the faculty at the Universidad Nacional de Córdoba he spent several years working at the Universidad Nacional de Río Cuarto, Argentina. Dr. Preidikman is a member of the IEEE, the American Institute of Aeronautics and Astronautics, the American Academy of Mechanics, and the Society for Industrial and Applied Mathematics. He is the author of more than 50 technical and scientific papers and of more than 160 conference papers. His current areas of research are in the fields of computational mechanics, numerical methods in engineering, unsteady and nonlinear aeroelasticity, flapping wings, bioinspiration and biomimetics.

Cristian Guillermo Gebhardt is Associate Professor in the Department of Structures at Córdoba National University of. He obtained his degree as Mechanical-Aeronautical Engineer from the Aeronautical Institute University in 2005. During 2006 he worked as a design engineer in the Department of Wind Energy at IMPSA. He obtained his PhD degree from Córdoba National University in 2012. He received important awards for his research focused on wind energy; among them, the 'Green Talents Award' for outstanding young scientist in 2011, awarded by the German Ministry of Education and Research. His current research interest includes structural mechanics, multi-body system dynamics, aerodynamics, aeroelasticity and wind energy

Julio César Massa is Professor in Structures Department of Córdoba National University in Argentina. He graduated as a Mechanical Engineer in Córdoba University in 1972 and received a Master Degree from Virginia Polytechnic Institute and State University in 1985. He has 40 years experience in teaching and researching in Córdoba University and he was also Professor at Río Cuarto National University from 1976 to 2010. His fields of research are Estructural Dynamics and Mechanical Design, areas where he has participated in many research projects.